

Application of Artificial Neural Networks (ANN) to Predict Geomechanical Properties of Asmari Limestones

M. Razifard¹, M. Khamechian^{1*}, M.R. Amin Naseri²

1) Department of Engineering Geology, Tarbiat Modares University, P.O. Box 14115-175, Tehran, Iran

2) Department of Industrial Engineering, Tarbiat Modares University, P.O. Box 14115-143, Tehran, Iran

E-mail address: mahdirazi.1982@gmail.com

*Corresponding Author

Abstract

A number of common laboratory rock mechanics tests are carried out in all geotechnical projects such as dams, to determine parameters such as porosity, density, water absorption, sonic velocity, Brazilian tensile strength, uniaxial compressive strength, and triaxial compressive strength. In this paper, data obtained from two dams in Asmari Formation including Khersan 1 and Karun 4 - both located in Chahar-Mahal Va Bakhtiari Province, Iran - have been subjected to a series of statistical analyses. Then, using Multivariate Linear Regression (MLR) and Artificial Neural Networks values of UCS, E, C, and ϕ were predicted using the input parameters including depth, compression ultrasonic velocity, porosity, density, and Brazilian tensile strength. The designed ANN in this research was a feedforward backpropagation network which is powerful tool to solve prediction problems. Designed network had two hidden layer (hidden layer 1: 18 neurons and hidden layer 2: 20 neurons). Via comparing designed MLR and ANN models, it was revealed that ANNs ($R^2_{UCS} = 0.91$, $R^2_E = 0.87$, $R^2_C = 0.78$, $R^2_{\phi} = 0.61$) are more efficient than MLR models ($R^2_{UCS} = 0.69$, $R^2_E = 0.69$, $R^2_C = 0.66$, and $R^2_{\phi} = 0.50$) in predicting strength and shear parameters of the intact rock. Also, to enhance the credibility of this study, some extra tests were carried out to evaluate the efficiency of network designed for prediction of strength parameters. The results obtained from this network were as: $R^2_{UCS} = 0.85$, $R^2_E = 0.81$.

Keywords: Artificial Neural networks (ANN), Feedforward Backpropagation; Multivariate Linear Regression (MLR); Asmari Formation; Uniaxial Compressive Strength (USC); Modulus of Elasticity (E); Cohesive Strength (C); ϕ (Internal Friction Angle)

1. Introduction

Dams are among the most important geotechnical structures constructed in the arid and semi-arid areas such as Iran, where a significant number of dams are during the last three decades. A noticeable number of dams are in Asmari Formation, which belongs to Oligocene to Miocene time. In many of geotechnical projects uniaxial compressive strength (UCS), static modulus of elasticity (E) of the intact rock material, c , and ϕ are required to be measured; however, it is not always possible to obtain suitable specimens from highly fractured and/or weathered rocks for this purpose (Tiryaki 2008).

For many years, the uniaxial compressive test has been the main quantitative method to determine the strength parameters of intact rock, i.e. uniaxial compressive strength (UCS) and static modulus of elasticity (E). This test results are directly applicable to studies concerning underground and surface mining, slope stability, drilling and blasting, and mechanical rock excavation (Tiryaki 2008). UCS is regarded among the input parameters for rock mass characterization and classification. On the other hand, E is a property of rock materials which measures how closely they approximate to the ideal elastic material (Farmer 1968; Jumikis 1979). These two parameters are also important in determining the breakage behavior of rocks under the action of rock cutting picks in mechanical excavation (Tiryaki & Dikmen 2006).

The procedure for Uniaxial Compressive Test has been standardized by both the American Society for Testing and Materials (ASTM 1984) and the International Society for Rock Mechanics (Brown 1981). Although the method is relatively simple, it is time consuming and expensive; besides, it requires well prepared rock cores. As a consequence, indirect tests -such as Schmidt rebound number, point load index, impact strength, and sound velocity - are often applied to predict the UCS and E. These tests are easier to be carried out since they necessitate less or no sample preparation and the testing equipment is less

complicated. Furthermore, they can be used easily in the field. Therefore, it can be resulted that, compared to the uniaxial compression test, indirect tests are simpler, faster, and more economical (Kahraman 2001). Within the last years, a large number of equations have been proposed to predict UCS and E from the other parameters. Some of these relationships are summarized in Table 1.

The relationships between the rocks parameter are not always linear and a plenty of factors control their behavior. This complexity of behavior calls for using a more sophisticated method. In the last few years, Artificial Neural Networks (ANN) and fuzzy logic have been used to establish predictive models for UCS and E for rock engineering applications (Sonmez et al. 2004). ANN models have also been used in many other geotechnical and geological applications (e.g., Landslide susceptibility mapping (Khamehchiyan et al. 2011)). Some other applications of ANNs are summarized in Table 2.

The purpose of this study is to analyze the results obtained by designing ANN's and MLR models to predict UCS, E, C, and ϕ . The data used in this study were gathered from the tests performed in two geotechnical projects, including dams of Khersan 1 and Karun 4, as well as the data obtained from the tests done by the author in Tarbiat Modares University of Tehran, Iran. It is worth to mention that the most of previous studies have just used ANNs to predict UCS and E, while in this research C and ϕ were investigated as well as UCS and E. besides, a set of extra tests were conducted by the researcher to evaluate efficiency of the network and enhance credibility of the study.

2. Geological setting

Dataset used in this research were taken from two projects: Khersan Dam 1 and Karun Dam 4. These projects are both located in Asmari Formation in Zagros fold region. The geological evidence suggests that Zagros region was a part of a passive continental margin, which subsequently underwent rift-

Table 1. the equations proposed for prediction of UCS and E from simpler tests

References	Proposed Equation	R	Rock type	R _L	Applied Test	
(Aufmuth, 1973)	$UCS=0.33*(RL*\rho)^{1.35}$	0.8	different lithologies	10 - 54	Schmidt Hammer	
	$Et=4911.84*(RL*\rho)^{1.06}$	0.75				
Kahraman (1996) in (Yilmaz and Sendir, 2002)	$UCS=0.00045*(R_N*\rho)^{2.46}$	0.96	different lithologies			
Gokceoglu (1996) in (Yilmaz and Sendir, 2002)	$UCS=0.0001R_N^{3.27}$	0.84	Marl			
(Xu et al., 1990)	$UCS=2.98*e^{(0.06 * R_L)}$	0.95	Mica-schist	17 - 53		
	$Et=1.77*e^{(0.07 * R_L)}$	0.96				
	$UCS=2.99*e^{(0.06 * R_L)}$	0.91	Prasinite	21-64		
	$Et=2.71*e^{(0.04 * R_L)}$	0.91				
	$UCS=2.98*e^{(0.063 * R_L)}$	0.94	Serpentinite			
	$Et=2.57*e^{(0.03 * R_L)}$	0.88				
	$UCS=3.78*e^{(0.05 * R_L)}$	0.93	Gabbro			
	$Et=1.75*e^{(0.05 * R_L)}$	0.95				
	$UCS=1.26*e^{(0.52 * R_L * \rho)}$	0.92	Mudstone			
	$Et=0.07*e^{(0.31 * R_L * \rho)}$	0.89				
(Deere and Miller, 1966)	$UCS=9.97*e^{(0.02 * R_L * \rho)}$	0.94	different lithologies	23-59		
	$Et=0.19*RL*\rho^2 - 7.87$	0.88				
(Katz et al. 2000)	$UCS=2.21*e^{(0.07 * R_N)}$	0.96	Limestone and sandstone	24-73	Load Point Index	
	$Et=0.00013*R_N^{3.09}$	0.99				
(D'Andrea et al. 1984)	$UCS = 15.3I_{S50} + 16.3$		different lithologies			
(Broch and Franklin, 1972)	$UCS = 24I_{S50}$					
(Bieniawski, 1975)	$UCS = 23I_{S50}$					
(Hassani et al. 1980)	$UCS = 29I_{S50}$					
(Goktan, 1988)	$UCS = 0.036V_p - 31.18$		coal			Ultrasonic Velocity
(Kahraman, 2001)	$UCS = 9.9V_p^{1.21}$	0.83	Serpentine			
(Hobbs, 1964)	$UCS = 53ISI - 2509$		different lithologies			Impact Strength Test
(Goktan, 1988)	$UCS = 0.095ISI - 3.667$		different lithologies			

Abbreviations:

UCS: Uniaxial Compressive Strength (MPa); E_t: tangent Young's modulus (GPa) at 50% of UCS; ρ: density (gm/cm³); R_L and R_N: rebound values for L and N hammers; Is50: point load index (Is) when the sample diameter is 50 mm; V_p: Compressive wave ultrasound velocity (m/s); ISI: Impact Strength Index; r: Correlation coefficient

Table 2. various applications of Neural Networks in geotechnical engineering

References	Application
(Khamehchiyan et al. 2011)	Landslide susceptibility mapping
(Finol et al., 2001)	Predicting petrophysical rock parameters
(Fowell, 1970)	Assessing the machineability of rocks
(Kahraman et al., 2006)	Predicting sawability of the carbonate rocks
(Kalantary et al., 2009)	Investigate the applicability of the correction factors in Su-NSPT
(?anakci and Pala, 2007)	Prediction tensile strength of basalt
(Tiryaki, 2008)	Predicting the cuttability of rocks by drag tools
(Ahmad et al., 2007)	Estimation of kinematic soil pile interaction response parameters
(Gomez and Kavzoglu, 2005)	Assessment of landslide susceptibility
(Wang et al., 2007)	Calculation of embankment settlement
(Moosavi et al., 2006)	Modeling the cyclic swelling pressure of mudrock

ing during the Permo-Triassic and collision during the Late Tertiary (Stocklin 1974). Zagros fold-thrust belt lies on the northeastern margin of the Arabian plate and has been divided into NW-SE trending structural zones (imbricated and simply folded belt) parallel to the plate margin separated by major fault-zones such as the High Zagros and Mountain Front

Faults (Jafarzadeh and Hosseini-Barzi 2008).

Asmari Formation, which is one of the best-known carbonate reservoirs in the world - was deposited in the Oligocene-Miocene shallow marine environment of the Zagros foreland basin (Alavi 2004). Lithologically, the Asmari Formation consists of 314 m of limestones, dolomitic limestones, and argilla-

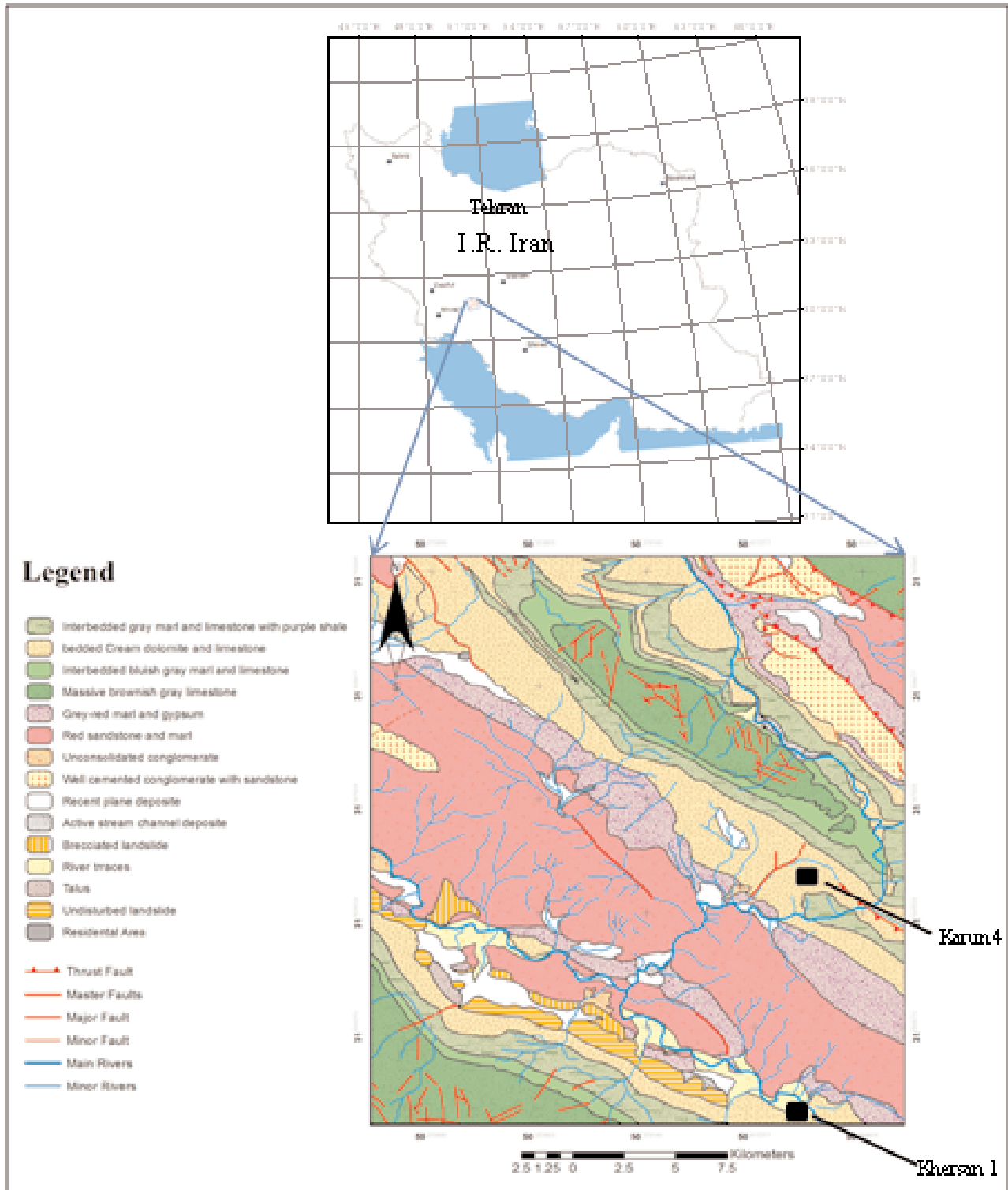


Figure 1. location of studied dams (indicated by black squares)

aceous limestones. In the south of Dezful embayment, its lithology changes into a mixed siliciclastic-carbonate deposit consisting of carbonate beds with several intervals of sandstone, sandy limestone and shale. This facies provides the Ahwaz Sandstone Member in some oil fields such as Ahwaz, Marun and Mansuri (Motiei 1993).

The studied area is located within the Izeh Zone which is a part of Zagros fold. Khersan 1 dam is located in 50 26 37 E and 31 30 10 N (Khersan 1) and can be accessed by Isfahan-Boroujen-Lordgan and then Lordgan-Monj-GhaleMadraseh roads; while Karun 4 is within the 50 28 00 E and 31 35 59 N and can be accessed by Isfahan-Boroujen-Lordgan and then LordganIzeh-roads. The location of these two dams is shown in (Fig. 1)

3. Data analysis

As previously mentioned, the main share of data used in this study were gathered from the tests carried out

on limestone cores extracted from two geotechnical projects (i.e., Khersan 1 and Karun 4 - performed in Asmari Formation (in Lordegan City, Iran). The tests were carried out in the laboratories of MahabQods Engineering Consultancy Company as well Tarbiat Modares University of Tehran, Iran. For all extracted cores (120) the tests including determination of ultrasonic wave velocity, special density (G_s), water absorption percentage ($w\%$), Brazilian Tensile Strength (T), uniaxial compressive strength, and triaxial compressive strength tests were performed. Table 2 introduces the basic descriptive statistics for the performed tests.

After descriptive statistical analysis, the original data were subjected to bivariate correlation to find out the relationships between UCS, E, C, and ϕ and other intact rock properties. These relationships are shown in (Fig. 2 and 3) and Table 4.

In the next step, to discover the distribution manner of the data set, a boxplot graph was created. As the

Table 3. Basic descriptive statistics for the original data set

	V_p (m/s)	G_s	Water absorption (%)	Brazilian Tensile Strength (MPa)	UCS (MPa)	E (GPa)	C (MPa)	Phi
Min	3578	2.26	0.2	2.0	20.0	3.9	8.0	18.7
Max	6380	2.85	15.2	14.0	175.0	43.0	45.0	46.0
Average	5003	2.57	8.2	5.6	78.2	18.6	24.60	36.7
Median	5131	2.59	8.4	4.8	77.1	17.7	23.96	39.4
Standard Deviation	756	0.13	3.5	2.7	36.4	10.1	8.42	7.2
Variance	571368	0.02	12.0	7.4	1327.5	102.5	76.65	52.4

Table 4. bivariate relationships between rock's intact strength parameters with its other parameters

	Depth	V_p	G_s	Water absorption	Brazilian Tensile Strength	UCS	E	C	Phi
Depth	1.00								
V_p	-0.45	1.00							
G_s	0.36	-0.61	1.00						
Water absorption	0.33	-0.29	0.53	1.00					
Brazilian Tensile Strength	0.32	-0.51	0.41	0.38	1.00				
UCS	0.32	0.42	0.51	-0.50	0.55	1.00			
E	0.30	0.24	0.38	-0.68	0.56	0.77	1.00		
C	0.45	0.58	0.61	0.44	0.69	0.59	0.49	1.00	
Phi	-0.13	-0.51	-0.48	-0.20	-0.30	0.13	0.20	-0.53	1.00

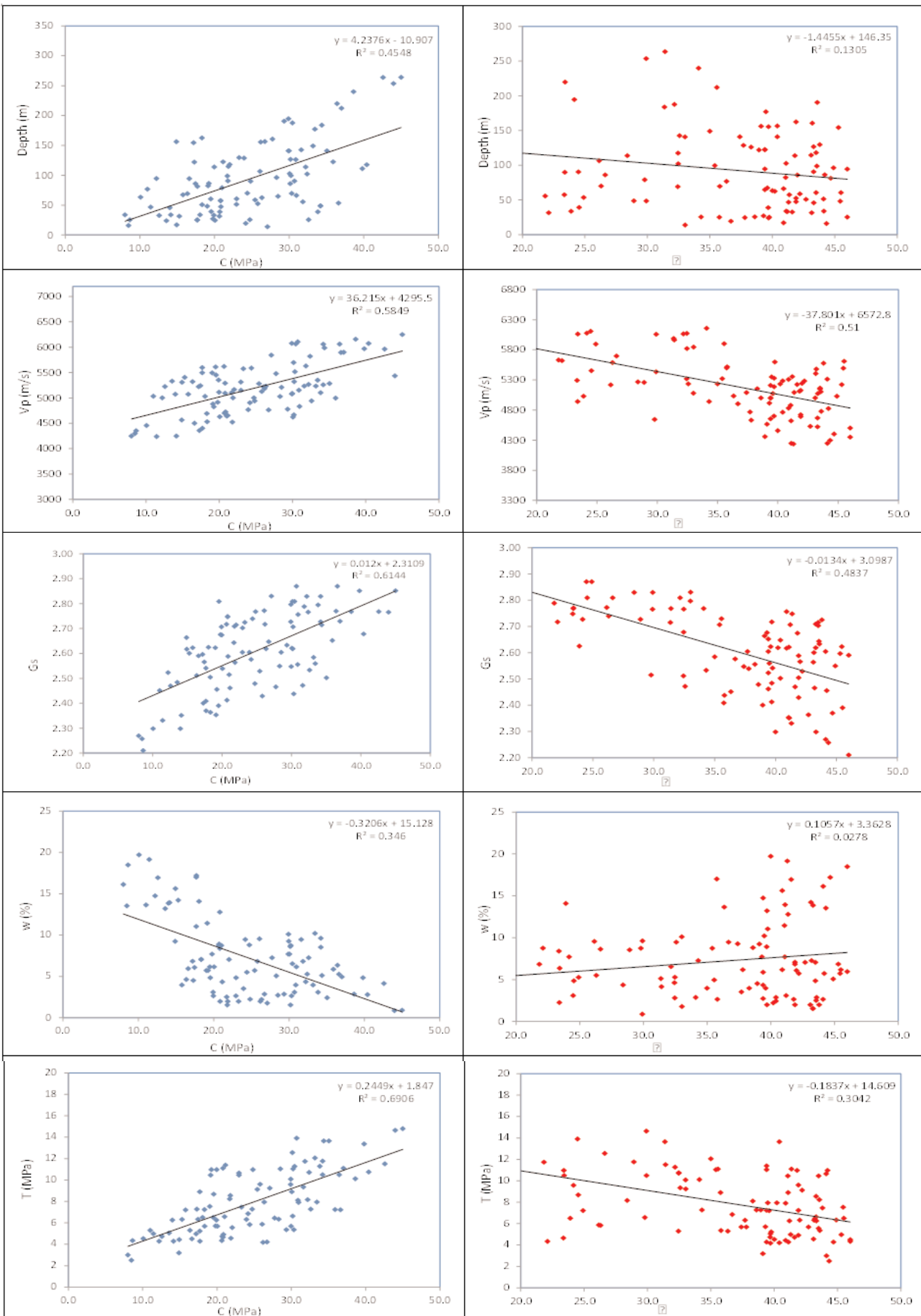


Figure 2. Relationship between C and ϕ with the other parameters of the intact rock

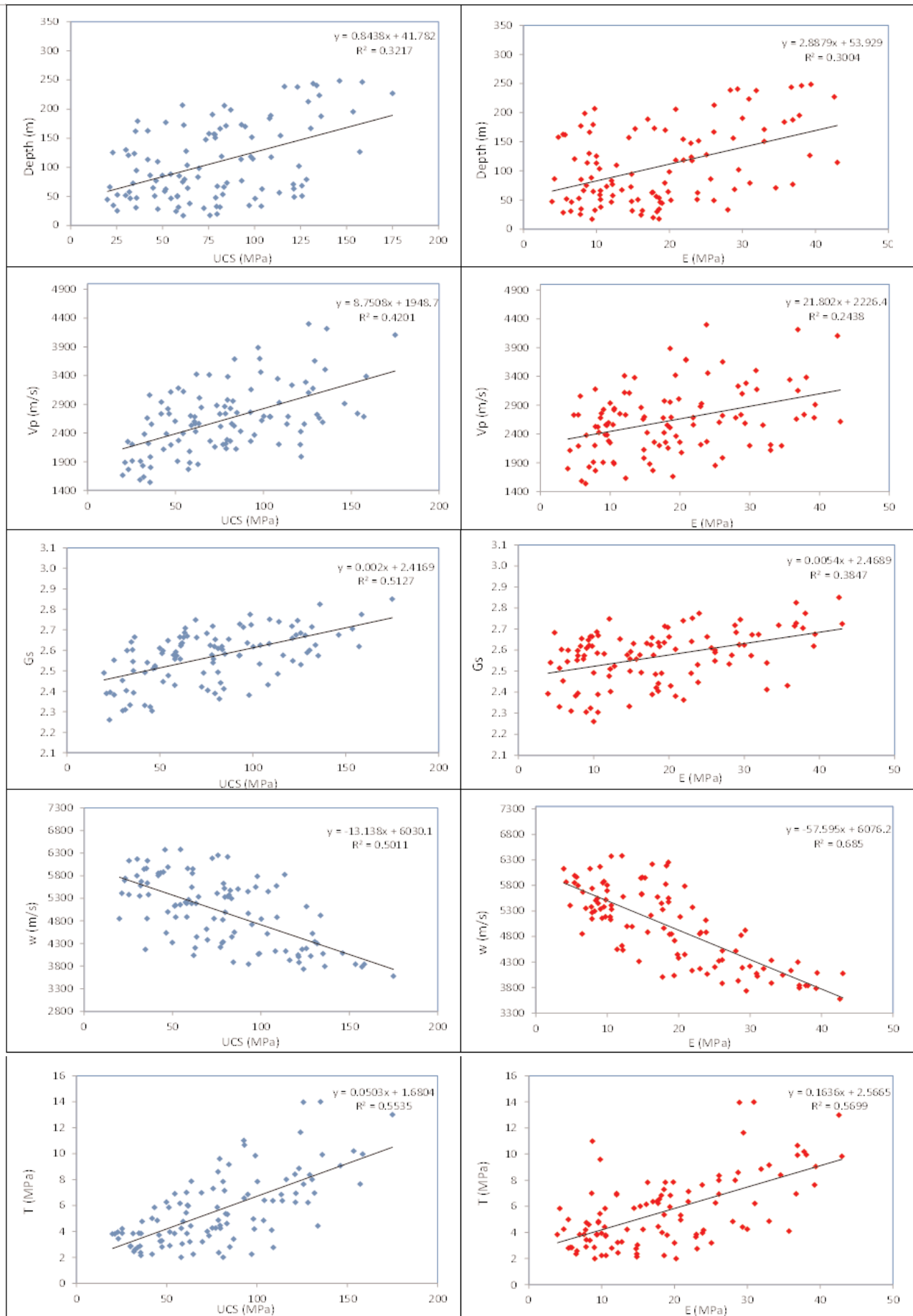


Figure 3. Relationship between C and ϕ with the other parameters of the intact rock

obtained data had different scales (for instance V_p data range were between 3578 and 6380, while G_s data varied between 2.26 and 2.85), they were normalized using the (1) to limit their values between 0 and 1.

$$\text{Normal data} = \frac{(A_i - A_{\min})}{(A_{\max} - A_{\min})} \quad (1)$$

Where,

A_1 : Unnormalized value

A_{\min} : The minimum value for a given parameter

A_{\max} : The maximum value for a given parameter

After normalization of the dataset, using the boxplot function a plot shown in Figure 4 was created (MATLAB 2008). From (Fig. 4), it can be implied that the outlier data are shown just in T (Brazilian tensile strength). Besides, the median in the boxes are almost (but not exactly) in the middle of box. So, MLR could offer a somehow good model to predict UCS and E.

4. Study method

Most of the problems in geology involve complex and interacting forces, which are impossible to isolate and study individually (Davis 1973). For this reason, MLR analysis was applied for the generalized model in this study because they allow us to consider changes in several properties simultaneously (Zorlu et al. 2008).

In statistics, the linear regression models are often in the following form:

$$y = \beta_0 + \beta_1 x_1 + \beta_2 x_2 + \beta_3 x_1 x_2 + \beta_4 x_1^2 + \beta_5 x_2^2 +$$

Where, a response variable y is modeled as a combination of constant, linear, interaction, and quadratic terms formed from two predictor variables x_1 and x_2 . Uncontrolled factors and experimental errors are modeled by. Given data on x_1 , x_2 , and y , regression estimates the model parameters β_j ($j = 1, \dots, 5$).

More general linear regression models represent the relationship between a continuous response y and a continuous or categorical predictor x in the form:

$$y = + \beta_1 f_1(x) + \dots + + \beta_p x_p(x) + \square$$

The response is modeled as a linear combination of (not necessarily linear) functions of the predictor,

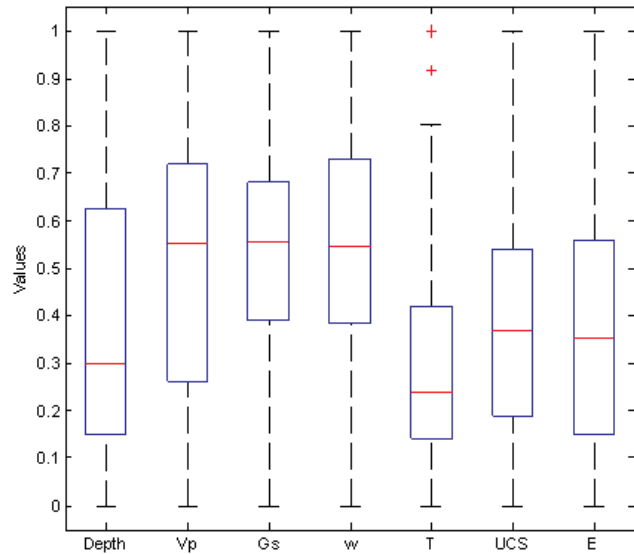


Figure 4. Boxplot of the normalized data set

plus a random error. The expressions $f_j(x)$ ($j = 1, \dots, p$) are the terms of the model. The β_j ($j = 1, \dots, p$) are the coefficients. Errors are assumed to be uncorrelated and distributed with mean 0 and constant (but unknown) variance (MATLAB 2008).

Another technique to predict the objective output parameters of this study is to use artificial neural networks. An artificial neural network is a massively parallel-distributed processor that has a natural propensity for storing experiential knowledge and making it available for use (Aleksander and Morton 1990). Neural networks are composed of simple elements operating in parallel inspired by biological nervous systems. As in nature, the connections between elements largely determine the network function. A neural network can be trained to perform a particular function by adjusting the values of the connections (weights) between elements.

ANNs basically simulate the behavior of the human brain. Because of its similarity to the human brain, even an ANN quite simple and small in size has some powerful characteristics in knowledge and information when compared to the human brain. Therefore an ANN can be a powerful tool for engineering applications (Ragip 2004).

Typically, neural networks are adjusted, or trained, so that a particular input leads to a specific target output. Fig.5 illustrates such a situation. There, the network

is adjusted, based on a comparison of the output and the target, until the network output matches the target. Typically, many such input/target pairs are needed to train a network (Howard and Mark 2000).

McCulloch and Pitts were the first who presented a formalized model of ANNs their network formed the basis for almost all later models (McCulloch and Pitts 1943). In the 1960s, Rosenblatt developed a simple-formalized model of a biological neuron based on the McCulloch-Pitts neurons, called perception. Rosenblatt's perceptions consist of "sensory" units connected to a single layer of McCulloch-Pitts neurons. In 1986, Rumelhart et al derived a learning algorithm for perception networks with hidden units. Their learning algorithm is called back-propagation and is now the most widely used learning algorithm (Rumelhart et al. 1986).

To the time, a wide variety of ANNs have been reported in the literature. Each type of ANN has an advantage in different tasks. Neural networks have been trained to perform complex functions in various fields, including pattern recognition, identification, classification, speech, vision, and control systems (Howard and Mark 2000).

4.1. Artificial neural networks structure

Fig. 6 illustrates a single ANN unit known as neuron. Here the input vector p is represented by the solid dark vertical bar at the left. The dimensions of p are

shown below the symbol p in the figures as $R \times 1$. Thus, p is a vector of R input elements. These inputs post multiply the single row R column matrix W . A constant 1 enters the neuron as an input and is multiplied by a scalar bias b . The net input to the transfer function f is n - the sum of the bias b and the product Wp . This sum is passed to the transfer function f to get the neuron's output a , which in this case is a scalar. Having more than one neuron would cause the network output to be a vector.

A layer of a network is defined in the (Fig. 6). The layer includes the combination of the weights, the multiplication and summing operation (here realized as a vector product Wp), the bias b , and the transfer function f (Howard and Mark 2000).

The initial weights of ANN strongly influence the

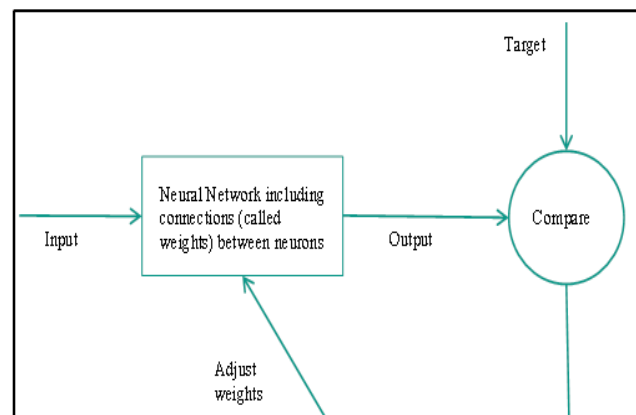


Figure 5. A schematic of a neural network system

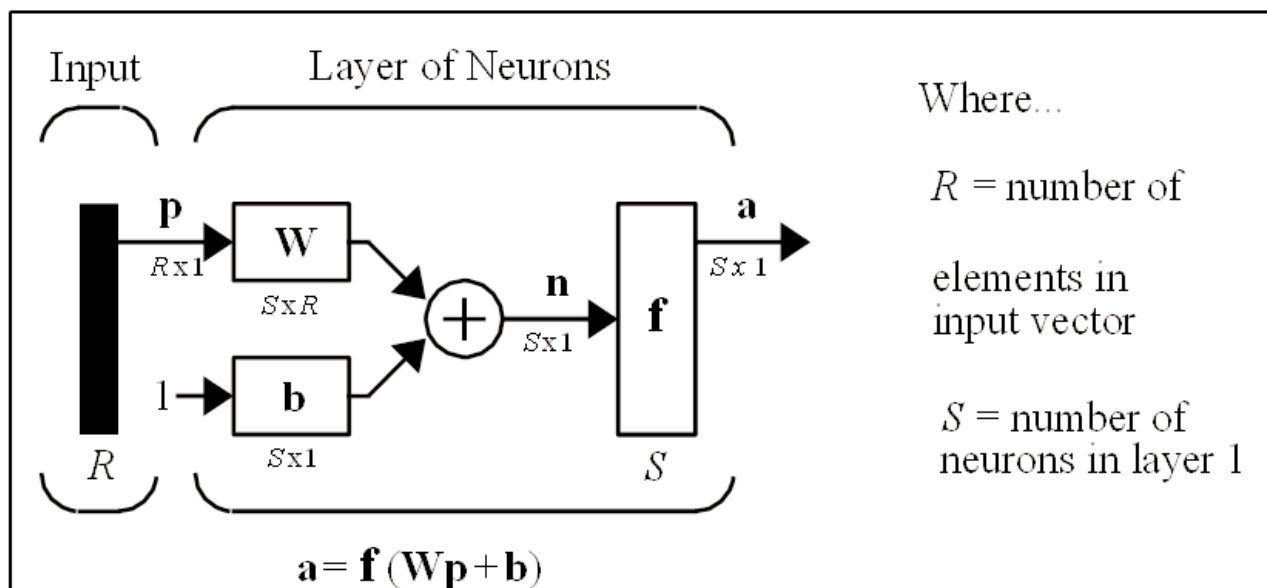


Figure 6. Mathematic model of a single ANN neuron

convergence of the BP learning rule, although (Gomez et al. 2002) donot believe this. Usually the weights are initialized at small random values. (Looney 1997) suggested values [-0.1, +0.1] or [-0.5, +0.5] while some other researchers proposed values [-0.25, +0.25] (Kavzoglu 2001). Another important parameter influencing the convergence of the model is the learning rate. In fact, there is not a general guideline for selecting a suitable learning rate, and in most of the cases, it is selected experimentally for each particular problem through trial and error approach (Khamehchiyan et al. 2011).

5. Results

In this paper, outputs of uniaxial compressive test (UCS and E) and triaxial compressive test (C and φ) were predicted using MLR and ANNs. For this goal, 4 linear regression as well as two ANNs were designed. The obtained results are as follows:

5.1. The results obtained by MLR models

In this research, using the SPSS18 software, 4 MLR models were developed to predict UCS, E, C, and φ. The best MLR model to predict these parameters was backward method in which the parameters are elimi-

nated one by one until reaching to an equation in which the parameters have the lowest significance value (0.0).

The results obtained by this process are summarized in Table 5. The final outputs of this method were equations (2), (3), (4), and (5) which predict UCS, E, C, and φ respectively:

$$UCS = 100.8 + 0.066 D - 0.015 V_p + 3.6 w + 3.91T$$

$$R^2 = 0.69$$

$$E = 83.1 + 0.021 D - 0.009 V_p - 10.64 G_s + 0.08 w + 0.92T$$

$$R^2 = 0.69$$

$$C = -7.2 + 0.005 V_p - 0.99 w + 0.93T$$

$$R^2 = 0.66$$

$$\phi = 168.2 + 0.005V_p - 43.9G_s - 0.79w - 0.56T$$

$$R^2 = 0.50$$

Where,

D: Depth (m), V_p : Compressive wavelength velocity (m/s), G_s : Special gravity, w: Water absorption (%), T: Brazilian tensile strength (MPa), UCS: Uniaxial compressive strength (MPa), E: elastic modulus of Young (GPa), C: cohesive strength, and φ: internal friction angle.

5.2. The results obtained by ANN

To predict outputs of uniaxial and triaxial compres-

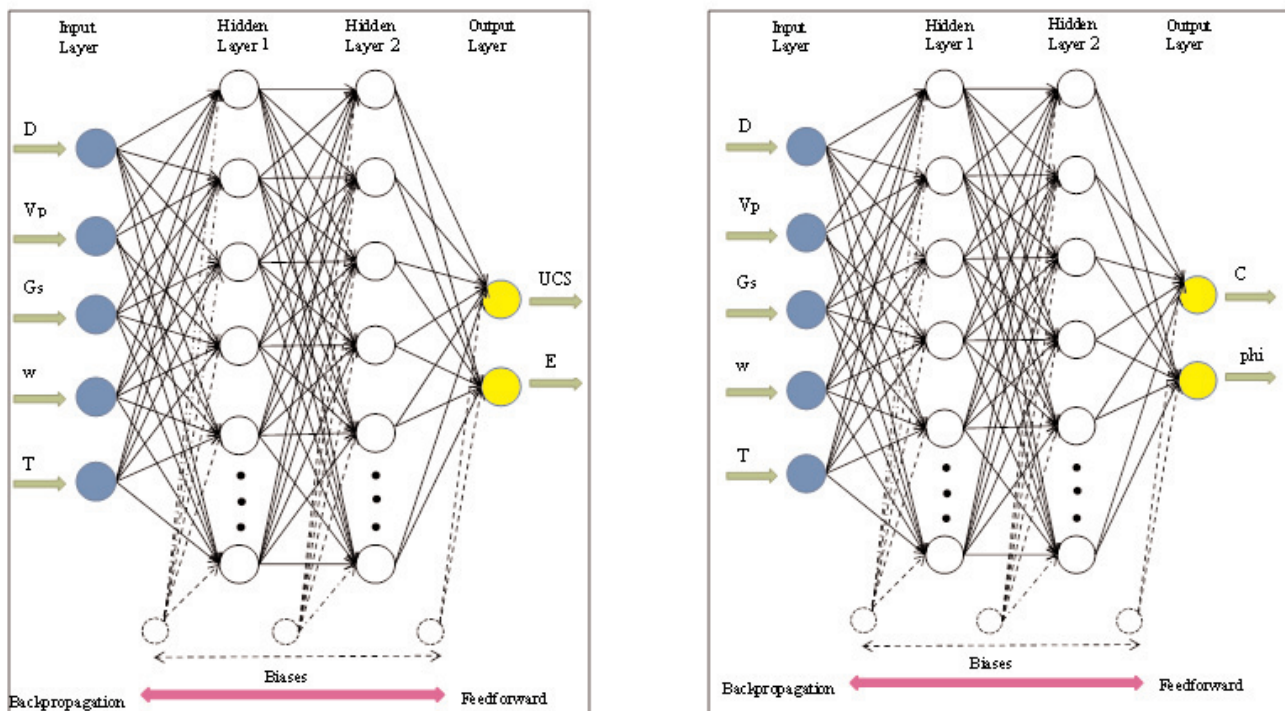


Figure 7. A diagrams of the designed ANNs to predict UCS, E, C, and φ

Table 5. the result obtained from MLR

Predicted Parameter	Model		Unstandardized Coefficients		Sig.	R ²
			B	Std. Error		
UCS	1	(Constant)	101.85	7.54	0.00	0.69
		Depth (m)	0.07	0.00	0.00	
		V _p (m/s)	-0.02	0.00	0.00	
		G _s	-0.35	2.53	0.89	
		Water absorption (%)	3.60	0.08	0.00	
	Tensile Strength (MPa)	3.92	0.09	0.00		
	2	(Constant)	100.85	2.36	0.00	0.69
		Depth (m)	0.07	0.00	0.00	
		V _p (m/s)	-0.02	0.00	0.00	
		Water absorption (%)	3.60	0.08	0.00	
Tensile Strength (MPa)		3.92	0.09	0.00		
E	1.00	(Constant)	83.10	2.22	0.00	0.69
		Depth (m)	0.02	0.00	0.00	
		V _p (m/s)	-0.01	0.00	0.00	
		G _s	-10.64	0.74	0.00	
		Water absorption (%)	0.08	0.02	0.00	
		Tensile Strength (MPa)	0.92	0.03	0.00	
C	1	(Constant)	-20.73	17.91	0.25	0.66
		Depth (m)	0.004	0.01	0.65	
		V _p (m/s)	0.005	0.00	0.00	
		G _s	5.91	7.67	0.44	
		Water Absorption (%)	-0.90	0.25	0.00	
		Brazilian Tensile Strength (MPa)	0.92	0.19	0.00	
	2	(Constant)	-20.92	17.83	0.24	0.66
		V _p (m/s)	0.005	0.00	0.00	
		G _s	6.12	7.62	0.42	
		Water Absorption (%)	-0.92	0.24	0.00	
		Brazilian Tensile Strength (MPa)	0.91	0.19	0.00	
	3	(Constant)	-7.20	5.05	0.16	0.66
		V _p (m/s)	0.005	0.00	0.00	
		Water Absorption (%)	-0.99	0.23	0.00	
		Brazilian Tensile Strength (MPa)	0.93	0.19	0.00	
	1	(Constant)	168.70	24.27	0.00	0.51
		Depth (m)	0.01	0.01	0.38	
		V _p (m/s)	0.00	0.00	0.05	
		G _s	-44.52	10.39	0.00	
		Water Absorption (%)	-0.74	0.33	0.03	
		Brazilian Tensile Strength (MPa)	-0.54	0.26	0.04	
	2	(Constant)	168.20	24.23	0.00	0.50
		V _p (m/s)	0.005	0.00	0.06	
		G _s	-43.97	10.35	0.00	
		Water Absorption (%)	-0.79	0.33	0.02	
Brazilian Tensile Strength (MPa)	-0.56	0.25	0.03			

sive tests two ANNs were designed and several types of ANN (e.g., Multilayer Perceptron, Modular Neural Network, Generalized Feedforward, and Multilayer Feedforward Backpropagation) were tested to predict

UCS and E. since the multilayer feed-forward network is the most commonly used network architecture with the back propagation algorithm (Demuth et al. 2006) and the results obtained from this networks

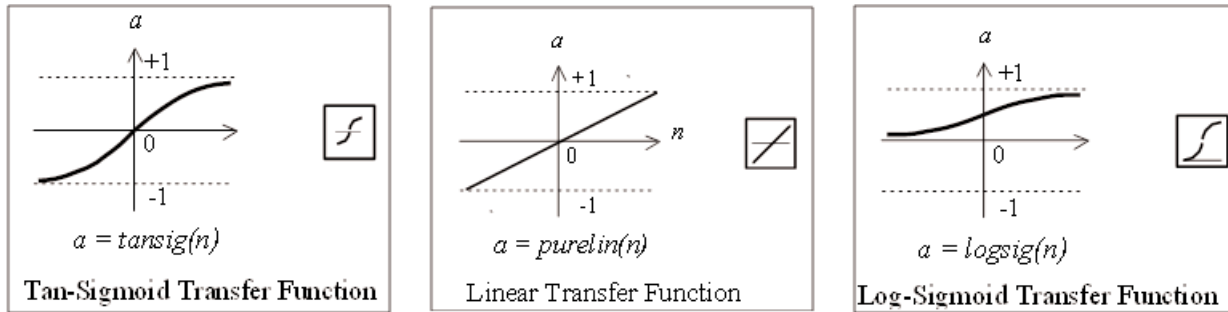


Figure 8. linear and log-sigmoid Transfer functions

yielded higher R^2 's, a backpropagation ANN architecture was used in this investigation. Two hidden layers were used for both designed networks, where 20 neurons in the first and 18 neurons in the second layer were for the first network (one which predicted UCS and E) and 18 neurons in first layer and 16 neurons in second layer for the second network (one which predicted C and ϕ). The initial investigations illustrated that when more hidden layers or fewer nodes in a single hidden layer are used, the network would not converge in the case there are a limited number of data. However, when more nodes in the hidden layer are utilized, the network will not be able to produce reasonably accurate predictions in the testing phase in spite of a highly improved convergence rate in the learning phase (Tiryaki 2008). The general view of the well-converging ANNs architecture is shown in (Fig. 7). Three bias neurons were also connected to the hidden and output layers. Each has a constant value of 1.

In this study, the applied transfer functions were: log-sigmoid (logsig), tangent-sigmoid (tansig), and linear (purelin) functions (Fig. 8).

5.2.1. Input and output data

In this study, 120 data sets were used. For input layer 5 parameters including depth (D), compressive ultrasonic velocity (V_p), special gravity (G_s), water absorption percent (w), and Brazilian tensile strength (T). Since two artificial neural networks were developed in this study to predict strength and shear parameters of the intact rock, there should be 4 output parameters including uniaxial compressive strength (UCS), elasticity modulus of Young (E), C, and ϕ to

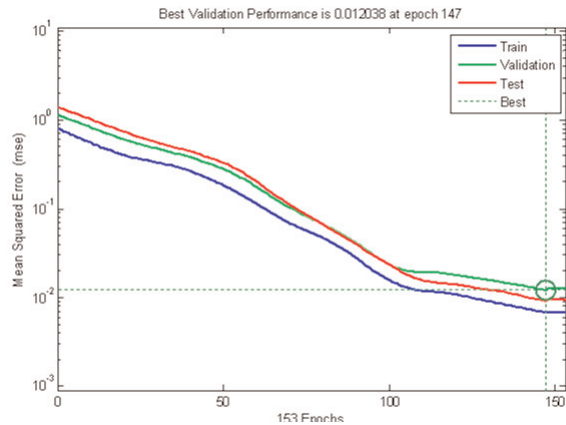


Figure 9. Network errors for two-hidden-neuron neural network

predict. The input dataset used in this study have different quantitative, so a normalization of data was required before presenting the input patterns to the ANN. In this paper, as previously mentioned, a linear normalization expression (1) was used to normalize the data to the values between 0 and 1.

5.2.2. Training of the ANN

The network can be trained for function approximation (nonlinear regression), pattern association, or pattern classification. The training process requires a set of examples of proper network behavior - network inputs p and target outputs t. During training the weights and biases of the network are iteratively adjusted to minimize the network performance function net. perform-Fcn. The default performance function for feedforward networks is mean square error (MSE) - the average squared error between the network outputs a and the target outputs t which can be estimated by (6).

$$MSE = \frac{1}{Q} \sum_{k=1}^Q e(k)^2 = \frac{1}{Q} \sum_{k=1}^Q (t(k) - a(k))^2 \tag{6}$$

Where t_k and a_k are target and obtained outputs, respectively.

Fig.9 shows one of the MSE versus epochs (the num-

ber of iterations) diagram.

By default of MATLAB toolbox, 85 percent of datasets are used as training and validation data. Thus, in this 100 dataset were used to train the network. The training and learning function used in this research were GDX (Gradient descent with momentum and adaptive learning rule backpropagation) and GDM (Gradient Descent with Momentum), respectively. Also, the learning rate was kept at 0.3 throughout the network training.

5.2.3. Testing designed ANN

5.2.3.1. Using the test data set

After the ANN was trained in the 100 training cases, it was tested to see how well it would predict UCS and E. In order to test the trained ANN, the remaining 20 data sets were used to simulate the network behavior. The final result showed that R^2 values are 0.91 and 0.87 for UCS and E, in network 1 and 0.78 and 0.61 for C and ϕ in the network 2 respectively. Fig. 10 to 13 compare the real values of UCS, E, C, and ϕ versus the predicted ones.

The properties of the final designed ANNs are summarized in Table 6 and Table 7.

5.2.3.2. Using the input data set produced by the author

To enhance credibility of this study and find out whether the designed network can predict the UCS and E from other data sets, 17 cores were subjected to laboratory tests in laboratory of TarbiatModares University. It must be mentioned, due to lack of enough cores and low accuracy of network 2, this process was just applied for testing network 1. Tests including determination of ultrasonic wave velocity (V_p), special density (G_s), water absorption percentage (w), Brazilian Tensile Strength (T), and Uniaxial Compressive Strength were performed on the cores. Then obtained inputs - Depth, V_p , G_s , w, and T - were introduced to the designed network (Table 6) using the sim function in MATLAB to simulated the values of UCS and E. The results obtained from the network and the real values of UCS and E had the R^2 values of 0.85 and 0.81, respectively. Fig. 14 compares real

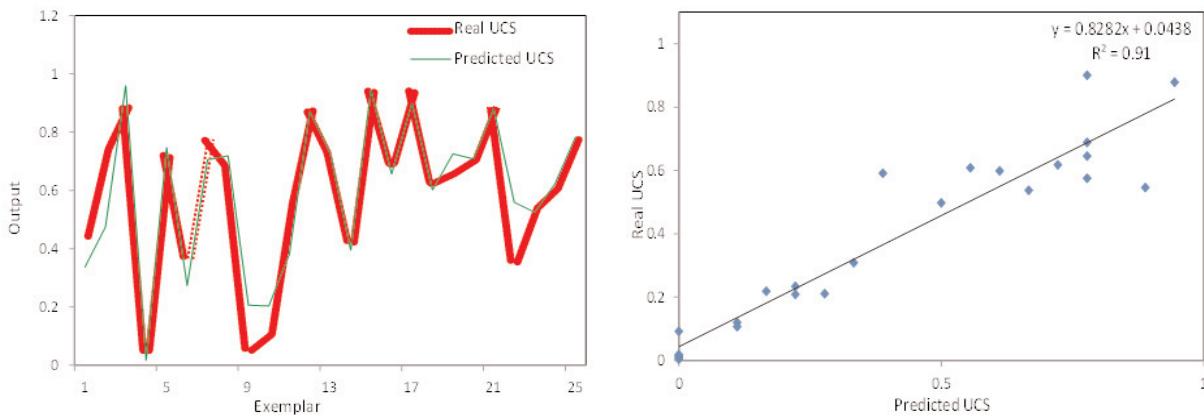


Figure 10. Predicted values of UCS versus Real values

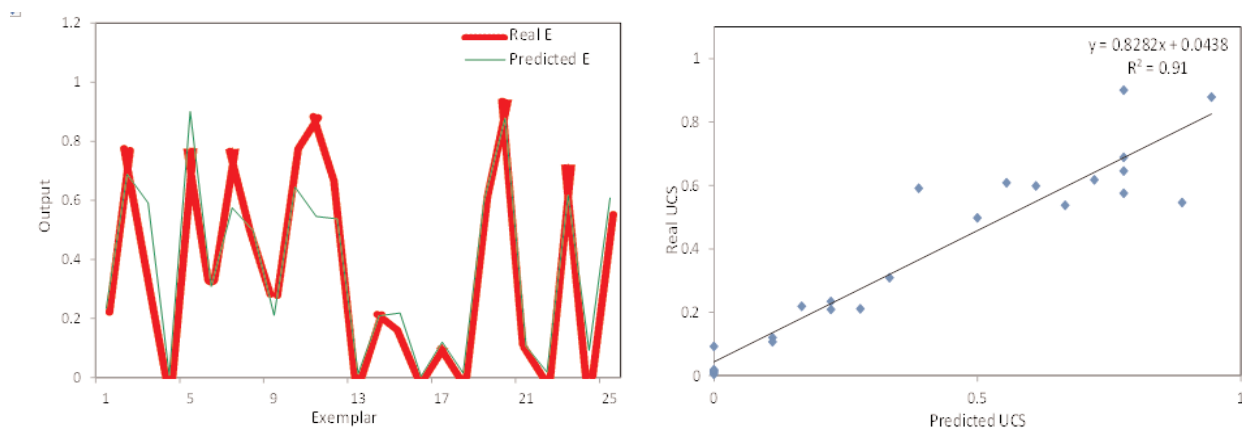


Figure 11. Predicted values of E versus Real values

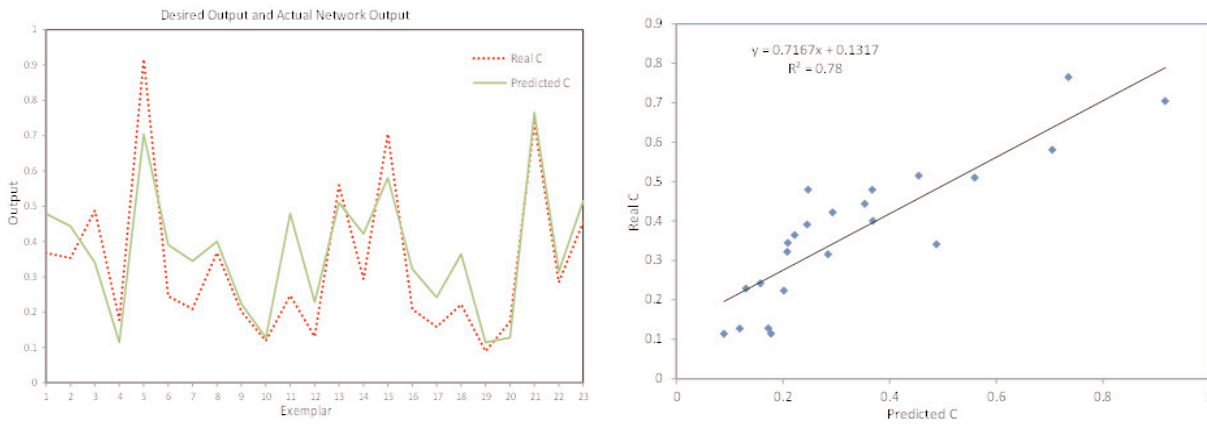


Figure 12. Predicted values of C versus Real values

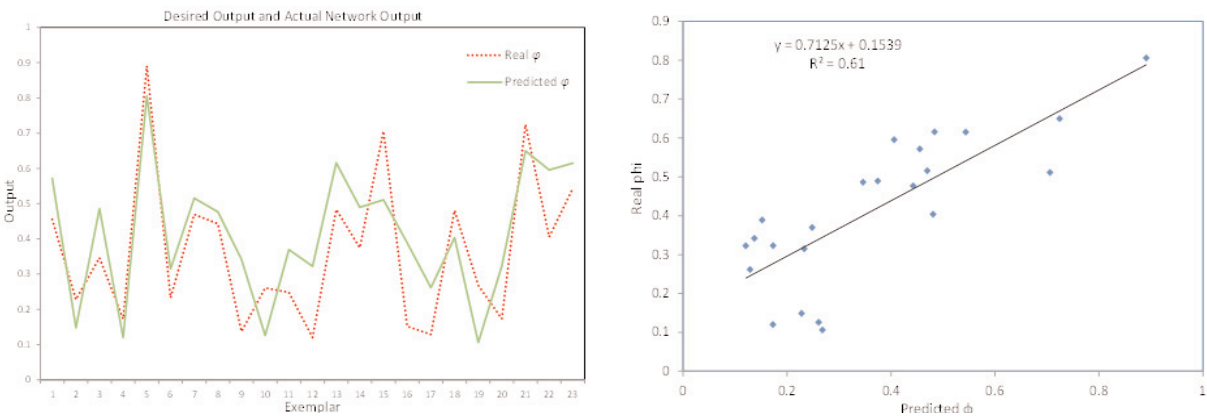


Figure 13. Predicted values of ϕ versus Real values

Table 6. Summary of the designed ANN for prediction of UCS and E

Network Type	Feed Forward Backpropagation ANN	
Number of hidden layers	2 layers	Layer 1: 18 neurons
		Layer 2: 20 neurons
Learning rate	0.3	
Training function	GDx (Gradient descent with momentum and adaptive learning rate backpropagation)	
Learning function	GDM (Gradient descent with momentum weight and bias)	
Number of epochs	253	
Minimum Square Error (MSE)	0.025	
Transfer function	Hidden layer 1	Log-sigmoid (logsig)
	Hidden layer 2	Log-sigmoid
	Output layer	Linear (purelin)

Table 7. Summary of the designed ANN for prediction of C and ϕ

Network Type	Feed Forward Backpropagation ANN	
Number of hidden layers	2 layers	Layer 1: 18 neurons
		Layer 2: 16 neurons
Learning rate	0.1	
Training function	GDx (Gradient descent with momentum and adaptive learning rate backpropagation)	
Learning function	GDM (Gradient descent with momentum weight and bias)	
Number of epochs	147	
Minimum Square Error (MSE)	0.045	
Transfer function	Hidden layer 1	Log-sigmoid (logsig)
	Hidden layer 2	tan-sigmoid
	Output layer	Linear (purelin)

values of UCS and E with those obtained predicted by the network. Also, data obtained from the laboratory tests are shown in Table 8.

6. Summary, conclusions, and suggestions for further studies

In this research, outputs of uniaxial compressive test (UCS and E) and triaxial compressive test (c and φ) were predicted using ANNs and MLR modeling. The study revealed that the applied ANN is a more powerful tool and can predict needed parameters with higher accuracy. According to the studies conducted by (Meulenkamp and Alvarez Grima 1999), (Geokceoglu and Zorlu 2004), (Tiryaki 2008), and (Singha et al. 2001; Zorlu et al. 2008), it can be

claimed the network designed in this research were efficient to predict UCS and E from the more simple parameters. However, according to the available database in this study, there was not any study on application of ANN's to predict C and φ. Nevertheless, it seems that the result obtained by both ANN's and MLR are not accurate enough. To enhance the accuracy of the results obtained from the ANN designed for triaxial test, it is suggested to use microscopic techniques to obtain textural parameters such as packing density (PD), grain area ratio (GAR), form factor (FF) of the grain, mean grain size (dmean), strong cement over matrix index (SMCI), strong cement over total cement (SCTC), and strong over weak contact (SOWC) may enhance the values

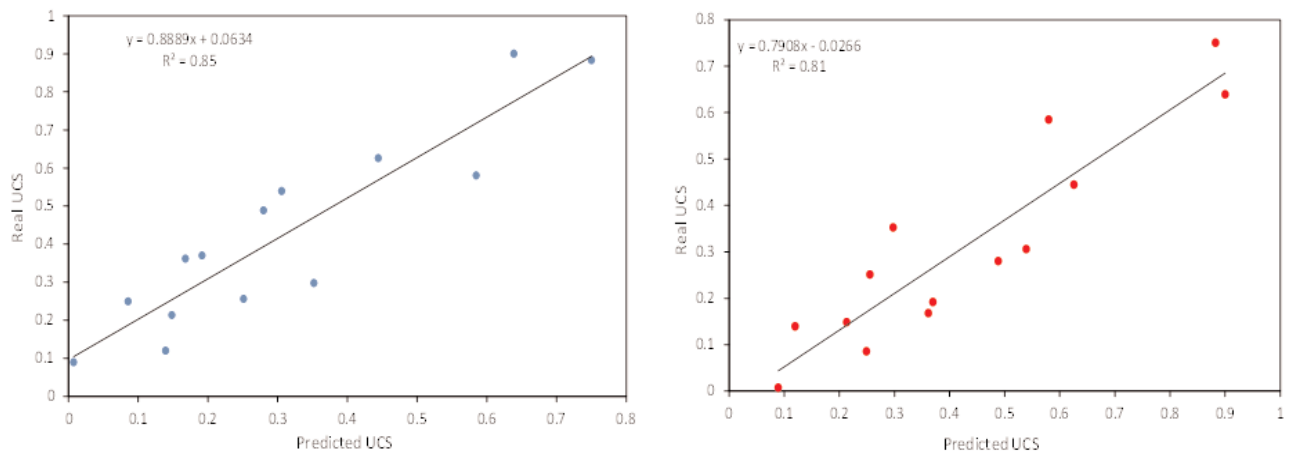


Figure 14. Comparison between real and predicted values of UCS and E using the laboratory data

Table 8. data set used to test the ANN obtained from laboratory tests

Sample No.	Depth (m)	V _p (km/s)	w (%)	G _s	T (MPa)	UCS (MPa)	E (GPa)
BH01A-01	79	4.68	2.02	2.51	8.5	77.6	23
BH01A-04	35	5.94	0.42	2.71	7.2	73.6	17.9
BH01A-08	49	4.92	0.57	2.49	5.2	69.6	8.4
BH05-02	38	4.27	0.32	2.48	9.5	57.2	23
BH05-03	184	4.52	1.11	2.5	9.1	49.4	7.9
BH05-04	190	5.23	2.3	2.69	6.9	66	6.7
BH05-05	173	6.15	1.19	2.72	5.7	46.8	9.3
BH05-06	47	5.42	0.31	2.62	6.5	54.6	19.8
BH07-01	49	4.21	2.05	2.44	3.7	28.3	5.9
BH07-02	96	6.08	0.55	2.69	3.4	17.7	19
BH07-03	180	5.08	0.57	2.42	3.9	24.8	10
KD01-01	128	5.21	0.21	2.51	9.1	88.3	10.6
KD01-02	155	6.1	0.36	2.71	9.9	115.4	13.3
KD01-03	349	5.51	0.61	2.45	7	85.7	21.9
KD01-04	30	5.73	0.32	2.68	9.7	96.1	17.1
KD01-05	238	4.98	0.73	2.48	12.9	101.3	29.5
KD26-03	102	4.22	0.47	2.47	5.1	81.6	29.3

of R^2 obtained for ANN designed for both triaxial and uniaxial tests (Jeng et al. 2004; Tamrakar et al. 2007). In general, the results obtained by this research can be summarized as:

1-Bivariate correlation analysis showed that Brazilian tensile strength ($R^2 = 0.45$), water absorption ratio ($R^2 = -0.59$), Brazilian tensile strength ($R^2 = 0.49$), and special gravity ($R^2 = -0.38$) are respectively the most reliable parameters to estimate UCS, E, C, and ϕ for the limestones used in this study.

2-The designed MLR models predicted UCS, E, C, and ϕ with R^2 of 0.69, 0.69, 0.66, and 0.50.

3- The designed ANN's predicted UCS, E, C, and ϕ with R^2 of 0.91, 0.87, 0.78, and 0.61.

4-Designed ANN was more successful for prediction of UCS in contrast to the other output parameters.

5-Using the test data set (those obtained from laboratory tests in Tarbiat Modares University), designed ANN predicted UCS and E with R^2 of 0.85 and 0.81.

6-Designed ANN models were more successful than MLR models to predict outputs of triaxial test (C and ϕ) and uniaxial test (UCS and E) using the mentioned input parameters.

Acknowledgment

Appendix

A-Definition and determination of petrographic parameters

A.1. Packing density

The packing density (PD), as defined by (Kahn 1956), is the ratio of the sum of the grain length encountered along a traverse across a thin section to the total length of the traverse, and PD can be expressed as eq.(7):

$$PD = \frac{\sum g_i}{t} \times 100\% \quad (7)$$

here g_i is the grain intercept length of the i th grain in the traverse as defined in Figure 15a; t is the total length of the traverse (eq.(8)).

A.2. Grain area ratio

$$GAR = A_g / A_t \quad (8)$$

ere A_g is the total area of all grains within a reference

area and A_t is the total area enclosed by the reference area boundary.

A.3. Grain contact

The GC, as defined by (Dobereiner and De Freitas 1986), is the ratio to its own total length of the length of contact a grain has with its neighbors and can be determined as eq.(9):

$$GC = \frac{\sum L_n}{L} \times 100\% \quad (9)$$

Where L_n = length of contact with other grain and L is the total length of boundary of a particular grain.

A.4. Form factor

Form factor can be defined as eq.(10):

$$FF = \frac{4\pi A}{L^2} \quad (10)$$

Where A is the area of a grain and L is the length of grain boundary. The values of FF range from close to 0, for very elongated or rough objects, to 1 for a perfect circle.

A.5. Mean grain size (d_{mean})

Mean grain size (d_{mean}) is defined as the average value of the diameters of all grains in a reference area, which represents the mean grain size.

A.5. cement over matrix index (SCMI)

SCMI that represents ratio of total strong cement over matrix in sandstone was calculated as eq.(11) (Tamrakar et al. 2007):

$$SCMI = \frac{(\% \text{Calsitic Cement} + \% \text{Siliceous Cement})}{(\% \text{Matrix})} \times 100 (\%) \quad (11)$$

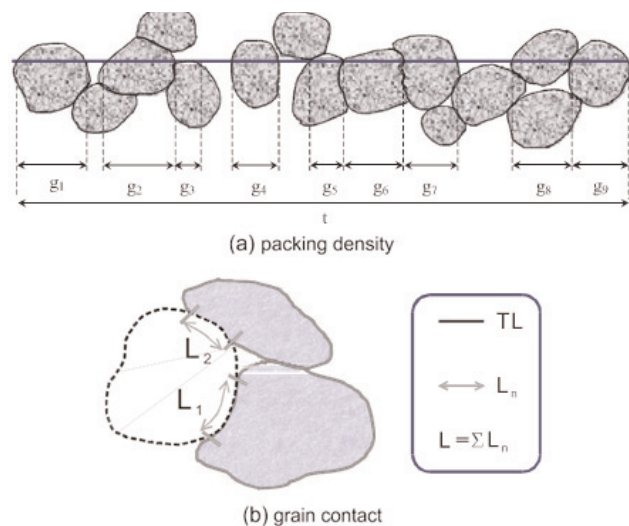


Figure 15. Schematic illustration of the definitions of packing density and grain contact ((Jeng et al. 2004))

A.6. Strong cement over total cement (SCTC)

SCTC can be defined as eq.(12):

$$SCTC = \frac{(\% \text{Calsitic Cement} + \% \text{Siliceous Cement})}{(\% \text{Total Cement})} \times 100 (\%) \quad (12)$$

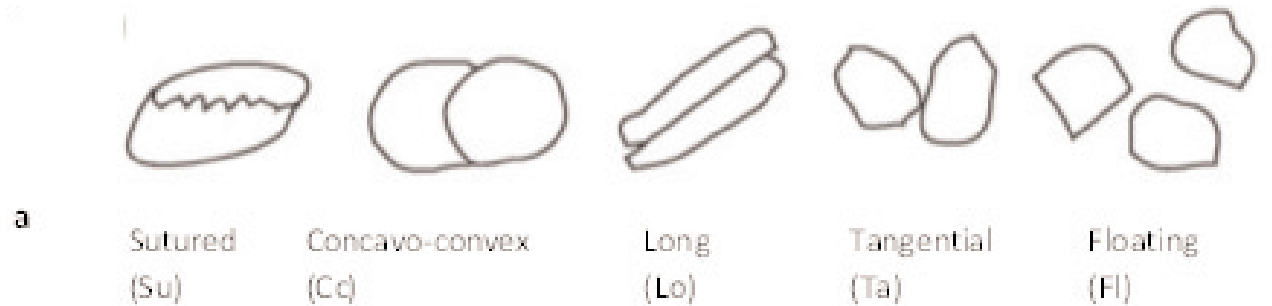
well the grains are interlocked and cemented and calculated using eq.(13):

$$SOWC = \frac{([S_u + (G-C)])}{([Ta + Lo + (G-V) + (G-M)])} \times 100 (\%) \quad (13)$$

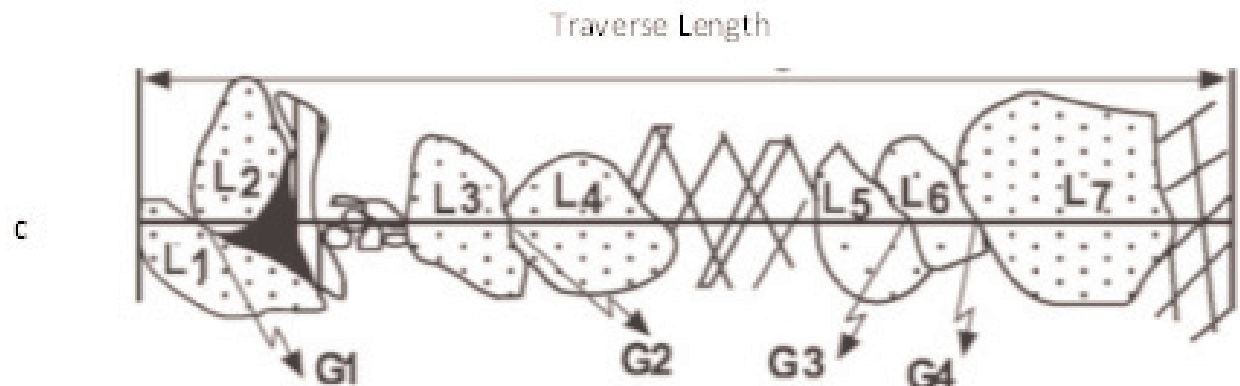
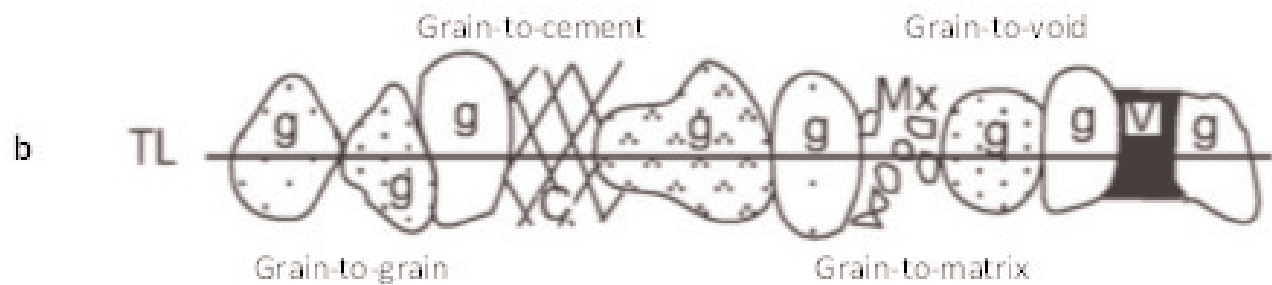
A.7. Strong over weak contact (SOWC)

Strong over weak contact (SOWC) represents how

Where the parameters are shown in (Fig. 16):



$$Pcc = \frac{(5.\%Su + 4.\%Cc + 3.\%Lo + 2.\%Ta + \%Fl)}{500} \cdot 100 (\%)$$



$$Packing Density, P_d = \frac{L_1 + L_2 + L_3 + L_4 + L_5 + L_6 + L_7}{Traverse Length} \times 100 (\%)$$

$$Packing Proximity, P_p = \frac{G_1 + G_2 + G_3 + G_4}{Number of contacts in the Traverse} \times 100 (\%)$$

Figure 16. Schematic diagrams showing contacts of grains in sandstones: (a) Contact types defined by (Taylor, 1950) and definition of consolidation factor, Pcc (Bell, 1978), (b) contact nature. TL; traverse length; g; grain, C; cement, Mx; matrix and V; void. (c) Definition of packing density, Pd and packing proximity, Pp (Kahn, 1956). L; length of each grain along the traverse line and G; number of grain-to-grain contact.

References

- Ahmad, I., Hesham El Naggar, M., Khan, A.N., 2007.** Artificial neural network application to estimate kinematic soil pile interaction response parameters. *Soil Dynamics and Earthquake Engineering* 27, 892-905.
- Alavi, M., 2004.** Regional stratigraphy of the Zagros fold-thrust belt of Iran and its proforeland evolution. *American Journal of Science* 304, 1-20.
- Aleksander, I., Morton, H., 1990.** An Introduction to Neural Computing. *Chapman and Hall*, London.
- ASTM, 1984.** Standard test method for unconfined compressive strength of intact rock core specimens. Soil and Rock, Building Stones: Annual Book of ASTM Standards 4.08. *Philadelphia, Pennsylvania: ASTM*.
- Aufmuth, R.E., 1973.** A systematic determination of engineering criteria for rocks. *Eng. Geol.* 11, 235- 245.
- Bell, F.G., 1978.** The physical and mechanical properties of the Fell Sandstones, Northumberland, England. *Engineering Geology* 12, 1-29.
- Bieniawski, Z.T., 1975.** Point load test in geotechnical practice. *Eng Geol* 9, 1-11.
- Broch, E., Franklin, J.A., 1972.** Point-load strength test. *Int J Rock Mech Min Sci* 9, 669-697.
- Brown, E.T., 1981.** Rock characterisation, testing and monitoring. ISRM suggested methods: Oxford: Pergamon Press, 1981, 211P. *International Journal of Rock Mechanics and Mining Sciences & Geomechanics Abstracts* 18, 109-109.
- Canakci, H., Pala, M., 2007.** Tensile strength of basalt from a neural network. *Engineering Geology* 94, 10-18.
- D'Andrea, D.V., Fisher, R.L., Fogelson, D.E., 1984.** Prediction of compression strength from other rock properties. *Colo Sch Mines Q* 59, 623-640.
- Davis, J.C., 1973.** Statistics and Data Analysis in Geology. Wiley, New York, N.Y. 550p.
- Deere, D.U., Miller, R.P., 1966.** Engineering classification and index properties for intact rock. Air Force Weapons Lab. *Tech. Report, AFWL-TR 65-116, Kirtland Base, New Mexico*.
- Demuth, H., Beale, M., Hagan, M., 2006.** Neural Network Toolbox for use with MATLAB. User's Guide Version 5. *The MathWorks, Inc*.
- Dobereiner, L., De Freitas, M.H., 1986.** Geotechnical properties of weak sandstone. *Geotechnique* 36, 79-94.
- Farmer, I.W., 1968.** Engineering Properties of Rocks. E. & F. N. Spon Limited.
- Finol, J., Guo, Y.K., Jing, X.D., 2001.** A rule based fuzzy model for the prediction of petrophysical rock parameters. *J. Pet. Sci. Eng* 29.
- Fowell, R.J., 1970.** Assessing the machineability of rocks. *Tunnelling and Underground Space Technology*, 251-253.
- Geokceoglu, C., Zorlu, K., 2004.** A Fuzzy Model to Predict the Uniaxial Compressive Strength and the Modulus of Elasticity of a Problematic Rock. *Engineering Application of Artificial Intelligence* 17, 61-72.
- Goktan, R.M., 1988.** Theoretical and practical analysis of rock rippability. *Ph.D. thesis, Istanbul Technical University*.
- Gómez, H., Kavzoglu, T., 2005.** Assessment of shallow landslide susceptibility using artificial neural networks in Jabonosa River Basin, Venezuela. *Engineering Geology* 78, 11-27.
- Gomez, H., Kavzoglu, T., Mather, P., 2002.** Artificial neural network application in landslide hazard zonation in the Venezuelan Andes. *Proceeding of Fifth International Conference on Geomorphology, Tokyo, Japan, 23-28 August Transactions of the Japanese Geomorphological Union*, 22 (4) C-76.
- Hassani, F.P., Scoble, M.J., Whittaker, B.N., 1980.** Application of point load index test to strength determination of rock and proposals for new size-correction chart. *Proceedings of the 21st US Symposium on Rock Mechanics, Rolla*, 543-564.
- Hobbs, D.W., 1964.** Rock compressive strength. *Colliery Eng* 41, 287-292.
- Howard, D., Mark, B., 2000.** Neural Network Toolbox For Use with MATLAB®. *Version 4*.
- Jafarzadeh, M., Hosseini-Barzi, M., 2008.** Petrography and geochemistry of Ahwaz Sandstone Member of Asmari Formation, Zagros, Iran: implications on provenance and tectonic setting. *Revista Mexicana de Ciencias Geológicas* 25, 247-260.
- Jeng, F.S., Weng, M.C., Lin, M.L., Huang, T.H., 2004.** Influence of petrographic parameters on geotechnical

- properties of tertiary sandstones from Taiwan. *Engineering Geology* 73, 71-91.
- Jumikis, A.R., 1979.** Rock Mechanics. Trans. *Tech. Publications, Clausthal, Germany.*
- Kahn, J.S., 1956.** The analysis and distribution of the properties of packing in sand-size sediments on the measurement of packing in sandstone. *The Journal of Geology* 64, 385-395.
- Kahrman, S., 2001.** Evaluation of simple methods for assessing the uniaxial compressive strength of rock. *International Journal of Rock Mechanics and Mining Sciences* 38, 981-994.
- Kahrman, S., Altun, H., Tezekici, B.S., Fener, M., 2006.** Sawability prediction of carbonate rocks from shear strength parameters using artificial neural networks. *Int. J. Rock Mech. Min. Sci* 43, 157-164.
- Kalantary, F., Ardalan, H., Nariman-Zadeh, N., 2009.** An investigation on the Su-NSPT correlation using GMDH type neural networks and genetic algorithms. *Engineering Geology* 104, 144-155.
- Katz, O., Reches, Z., Roegiers, J.C., 2000.** Evaluation of mechanical rock properties using a Schmidt Hammer. *Int. J. Rock Mechanics of Materials. Min. Sci.* 37, 723-728.
- Kavzoglu, T., 2001.** An investigation of the design and use of feedforward artificial neural networks in the classification of remotely sensed images. *PhD Thesis, University of Nottingham, School of Geography.*
- Khamehchiyan, M., Abdolmaleki, P., Rakei, B., 2011.** Landslide susceptibility mapping using backpropagation neural networks and logistic regression: The Sephidargole case study, Semnan, Iran. *Geomechanics and Geoengineering* 6, 237-250.
- Looney, C.G., 1997.** Pattern recognition using neural networks, theory and algorithms for engineering and scientists. *New York: Oxford University Press.*
- MATLAB, 2008.** Statistics Toolbox for Use with MATLAB.
- McCulloch, W.S., Pitts, W., 1943.** A logical calculus of the ideas immanent in neural nets. **Bulletin of Mathematical Biophysics** 5, 115-137.
- Meulenkamp, F., Alvarez Grima, M., 1999.** Application of neural networks for the prediction of the unconfined compressive strength (UCS) from Equotip hardness. *International Journal of Rock Mechanics and Mining Sciences* 36 29-39.
- Moosavi, M., Yazdanpanah, M.J., Doostmohammadi, R., 2006.** Modeling the cyclic swelling pressure of mudrock using artificial neural networks. *Engineering Geology* 87, 178-194.
- Motiei, H., 1993.** Stratigraphy of Zagros, in Hushmandzadeh, A. (ed.) *Treatise on the Geology of Iran: Tehran, Geological Survey of Iran.* 536.
- Ragip, I., 2004.** Prediction of fracture parameters of concrete by Artificial Neural Networks. *Engineering Fracture Mechanics* 71 2143-2159.
- Rumelhart, D.E., Hinton, G.E., William, R.J., 1986.** *Proceedings Parallel Distributed Processing.* In: Rumelhart DE, McClelland JL, editors. . Foundations, vol. . Cambridge: MIT Press 1.
- Singha, V.K., Singh, D., Singha, T.N., 2001. Prediction of strength properties of some schistose rocks from petrographic properties using artificial neural networks. *Int. J. Rock Mech. Min. Sci.* 38
- Sonmez, H., Tuncay, E., Gokceoglu, C., 2004.** Models to predict the uniaxial compressive strength and the modulus of elasticity for Ankara Agglomerate. *International Journal of Rock Mechanics and Mining Sciences* 41, 717-729.
- Stocklin, J., 1974.** Possible ancient continental margins in Iran, in Burk, C.A., Drake, C.L. (eds.), *The Geology of Continental Margins.* *New York, Springer,* 873-887.
- Tamrakar, N.K., Yokota, S., Shrestha, S.D., 2007.** Relationships among mechanical, physical and petrographic properties of Siwalik sandstones, Central Nepal Sub-Himalayas. *Engineering Geology* 90, 105-123.
- Taylor, J.M., 1950.** Pore space reduction in sandstone. *Bulletin of the American Association of Petroleum Geologists* 34, 701-716.
- Tiryaki, B., 2008.** Application of artificial neural networks for predicting the cuttability of rocks by drag tools. *Tunnelling and Underground Space Technology* 23, 273-280.
- Tiryaki, B., Dikmen, A.C., 2006.** Effects of rock properties on specific cutting energy in linear cutting of sandstones by picks. *Rock Mech. Rock Eng* 39 89-120.

Wang, Z.-l., Li, Y.-c., Shen, R.F., 2007. Correction of soil parameters in calculation of embankment settlement using a BP network back-analysis model. *Engineering Geology* 91, 168-177.

Xu, S., Grasso, P., Mahtab, A., 1990. Use of Schmidt hammer for estimating mechanical properties of weak rock. *6th International IAEG Congress, 1, 511 -519.*

Yilmaz, I., Sendir, H., 2002. Correlation of Schmidt hardness with unconfined compressive strength and Young's modulus in gypsum from Sivas (Turkey). *Eng. Geol.* 66, 211- 219.

Zorlu, K., Gokceoglu, C., Ocakoglu, F., Nefeslioglu, H., Acikalin, S., 2008. Prediction of uniaxial compressive strength of sandstones using petrography-based models. *Engineering Geology* 96, 141-158.